2nd URSI AT-RASC, Gran Canaria, 28 May – 1 June 2018

Tissue shrinkage in microwave ablation: *ex vivo* predictive model validation

L. Farina* (1,2), Y. Nissenbaum (3), S.N. Goldberg (3,4), and M. Cavagnaro(1)
(1) Dept. of Information Engineering, Electronics and Telecommunications, Sapienza University of Rome, Rome, Italy
(2) Translational Medical Device Laboratory & CURAM, National University of Ireland, Galway, Ireland
(3) Dept. of Radiology, Hadassah Hebrew University, Medical Center, Jerusalem, Israel
(4) Dept. of Radiology, Beth Israel Deaconess Medical Center, Boston, MA, USA

Abstract

Aim of the present study was to test and validate an *ex vivo* predictive model for the evaluation of the shrinkage occurring in hepatic tissue during a microwave thermal ablation procedure. Microwave ablation (N=134) was conducted with three different commercial devices on cubes of ex vivo liver (15–40 ± 2mm/side) embedded in agar phantoms. 50–60W was applied for 1–10 min duration. Pre- and post-ablation dimensions of the samples, as well as the extent of carbonization and coagulation were measured. The model results able to estimate the occurred contraction in presence of carbonization with good accuracy (>80% of the studied cases). The estimated error range resulted within the accuracy of the clinical practice.

1. Introduction

Microwave thermal ablation (MTA), a minimally-invasive thermal ablation therapy, is largely used to safely and effectively treat various solid tumors [1,2]. MTA exploits the interaction between a physical energy, i.e. an electromagnetic field at microwave (MW) frequencies, and the tissue to irreversibly damage the biological target through a temperature increase. When tissue temperature overcomes 55–60 °C, a denaturation process occurs in the cells, resulting in an irreversible cellular damage, i.e. thermal ablation [3]. In MTA, close to the radiating antenna the tissue temperature increases above 100 °C, and up to 120 °C, in the carbonized region [4]. Accordingly, the thermally ablated volume is usually made by a central carbonized area surrounded by a peripheral region of coagulated tissue. The thermally ablated volume depends on the exposure power and duration [5,6]. In the thermally ablated region, due to the high temperatures induced, a shrinkage up to about 30% occurs [8,9], which is clinically relevant [7]. Shrinkage can affect the estimation of the truly ablated volume leading to errors in the definition of the treatment planning, or in the evaluation of the post-procedural images [10]. Thus, the tissue contraction induced into the tissue during a MTA treatment needs to be taken into account to completely control the procedure and its results. To this end, investigation, modelling, and characterizing studies are needed.

Several *ex vivo* studies investigating biological tissue's shrinkage as a function of the temperature increase are reported in the literature [9, 11-14]. In particular, in [13] an *ex vivo* predictive model was presented. The analytical model links the dimensions of the thermally ablated area with the actual dimensions of the treated tissue, and considers different shrinkages for carbonized and for coagulated tissue. The model was developed based on only one type of commercially available microwave applicator, and tested only on it [13].
In the present work, a validation study of the shrinkage model proposed in [13] is reported: the model was tested on the data obtained treating *ex vivo* bovine liver tissue with three different commercially available MTA systems [14].

2. Materials and Methods

2.1 Experimental setup

Microwave thermal ablations (N=134) were conducted on *ex vivo* bovine liver cubic samples (side: 15, 20, 30 and 40mm± 2 mm). Samples were cut from larger blocks of tissue (up to 10 kg) obtained from a local slaughterhouse and stored in freezer at – 40 °C. Once defrosted and cut, the baseline tissue temperatures were measured, to insure initial conditions within the range 18–24 °C. The MTA applicator was inserted into the center of the cuboid sample in order to ensure that the radiating portion of the antenna was surrounded by the tissue. Then, the cube of tissue was inserted into an agar phantom (9%) to maintain electromagnetic and thermal continuity at the tissue boundaries. The dielectric phantom was prepared mixing distilled water (400 ml), agar powder (36 g, i.e. 9% of the water weight), sucrose (1.5 g) and sodium chloride (1.5 g). A glass beaker (500 ml, inner diameter 10 cm) was used to contain the phantom, with a central cavity precisely cut in the agar to insert the sample of tissue. This setup was then covered with additional agar diluted in saline solution to a height of 10–20 mm to ensure uniform field conditions [9,14].

2.2 MTA devices

The ablation procedures were performed with three different commercially available apparatuses for

microwave ablation all operating at 2.45 GHz [14]. In particular, the Acculis™ MTA System (AngioDynamics), the Amica™ system (HS Hospital Service S.p.A.), and the Emprint™ (Covidien) systems were considered. The commercial MTA systems used present different characteristics and design, and accordingly different settings are required [14]. The Acculis™ MTA system was operated supplying about 120W to water-cooled antennas for percutaneous insertion with a diameter of 1.8mm (Accu2i pMTA Applicator). It was acknowledged by the manufacturer that the power that effectively reaches the input port of the antenna is about 50% lower, due to losses of the coaxial cable connecting the generator to the antenna [15]. The AMICA™ system was operated supplying 60 W to 14-gauge water-cooled antennas with an active tip of 30mm (HS Amica probe 14 G). Both forward and reflected powers are continuously measured and displayed by the system; the losses of the connecting cable are constantly controlled, enabling to set the power effectively delivered to the antenna [16]. The Emprint™ system was operated supplying 100 W (maximum output power) to 13-gauge water-cooled antennas. As for the Acculis system, the coaxial cable connecting the generator to the antenna lowers the power effectively radiated into the tissue of about 40–50% [17]. The Emprint cooling system consists in water circulating into the entire antenna up to its tip. On the contrary in the Amica and Acculis applicators, the cooling liquid circulates only up to the choke section, i.e. about 20mm behind the antenna tip, and thus the actual "active tip" portion of the antenna is not cooled. Moreover, as reported by the manufacturer, the Emprint system continuously monitors and adapts electromagnetic field, tissue temperature, and wavelength to optimize the energy distribution into the tissue and provide a more spherical ablated region, and reduce tissue charring [17,18]. This results in a delayed appearance of carbonized tissue during the ablation procedure: a sizable carbonization is observable only after 5 min of ablation [14].

In all performed experiments, the MW power was set at the MW generator in order to supply an average power value of 50–60W at the antenna input port. Five different ablation times were tested from 1 min to 10 min. All the devices were used according to the manufacturer recommendations [14]. Distilled water at 10–16 °C was used to cool the applicators.

2.3 Data analysis

As sketched in Figure 1, radial ("d") and longitudinal ("ℓ") specimen dimensions before (D_N, L_N) and after heating (d_N, ℓ_N), including the extension of the carbonized (d_C, ℓ_C) and coagulated regions (d_A, ℓ_A), were measured with a ruler with an accuracy of 1 mm. To evaluate the post-ablation dimensions of the thermally ablated area, the tissue samples were cut along the antenna axis (Figure 1 right). The radial dimensions were measured at the antenna feed perpendicular to the antenna axis, whereas the longitudinal dimensions were measured at the center, along the observed antenna tract [14].

The predictive model

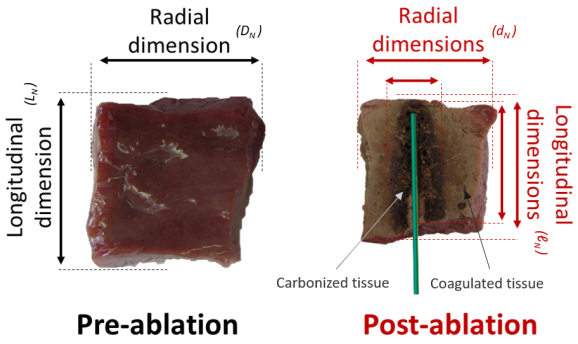

Figure 1. Schematic of the measured dimensions: cube sizes, extent of the coagulated and carbonised regions.

$$D_N = d_C / \alpha_{C,D} + d_A / \alpha_A \quad (1),$$

$$L_N = \ell_C / \alpha_{C,L} + \ell_A / \alpha_A \quad (2),$$

correlates the post- ablation dimensions with the pre-ablation ones through shrinkage factors. Three shrinkage factors were identified: two factors linked to the carbonized region, radially ($\alpha_{C,D}$= 0.63 ± 0.06) and longitudinally ($\alpha_{C,L}$= 0.76 ± 0.07) to the antenna axis, and one to the coagulated region (α_A= 0.88 ± 0.05), independent from the direction [13].

3. Results

The predictive model [13] was applied to the experimental results obtained with the Amica, Acculis and Emprint MTA systems, in order to evaluate the pre-ablation dimensions of the tissue samples starting from the post-ablation measurements, i.e. carbonized and coagulated region extensions, and final specimen sizes. The success rate of the model was evaluated comparing the analytically obtained values with the initial specimen sizes. A total uncertainty of 3 mm was considered for the model results, estimated on the experimental accuracy of 1 mm in the measurement of the extension of the different zones (carbonization, coagulation, and whole sample of tissue extensions). For the experiments conducted with the Acculis device, the mathematical model was able to predict the initial samples dimensions in 96 % of the cases (i.e. 115 over 120) in the radial direction and in 90 % of the cases (i.e. 54 over 60) in the longitudinal direction. For the experiments conducted with the Amica device, the mathematical model was able to predict the initial samples dimensions in 92% of the cases (i.e. 92 over 100 measures) in the radial direction and in 88% of the cases (i.e. 44 over 50) in the longitudinal direction. For the experiments conducted with the Emprint device, the mathematical model was able to predict the initial samples dimensions in 98% of the cases (i.e. 47 over 48 measures) in the radial direction and in 83% of cases (i.e. 20 over 24 measures) in the longitudinal direction. In the Emprint experiments, the success rate was estimated considering only the samples ablated for at least 5 min, i.e. accounting carbonized tissue [14], as foreseen by the model [13]. In the case of the Emprint system, in fact, within the first minutes of ablation (< 5 min), the tissue close to the antenna feed does not

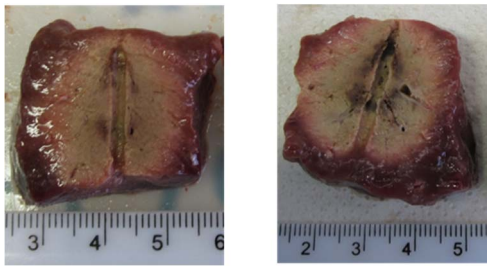

Figure 2. Appearance of cubes ablated for 1 min (left) and 2.5 min (right) with the Emprint™ system.

carbonize although its proximity to the energy source, as visible from Figure 2. Nevertheless, the shrinkage factor proposed in [13] for the only coagulated tissue (α_A) is not suitable to characterize the tissue in the only coagulated samples' case: an average contraction of 18 ± 5 % corresponding to a shrinkage factor of $\alpha_A = 0.82 \pm 0.05$, significantly lower with respect to the factor proposed in [13], can be evaluated independently from the direction for the samples ablated with the Emprint system for 1 and 2.5 min. The presence of traces of carbonization around the antenna feed let suppose that, in close proximity to the antenna feed, the increase of temperature due to the direct absorption of the electromagnetic field is limited by the active influence of the cooling system adopted by the Emprint system, and it possibly results in a temperature profile different from the exponentially decreasing observable instead in presence of carbonization, i.e. in presence of temperatures above 100 °C [14, 19].

Table I, II and III illustrate the average, minimum and maximum errors observed applying the model to the experimental data: the difference between the resulting analytical data and the measured initial dimensions of the samples is reported. The observed error range is [-3; 5] mm in the samples treated with the Acculis system (Table I), [-7; 4] mm in the samples treated with the Amica system (Table II), [-8; 3] mm in the samples treated with t he Emprint system (Table III). A negative value indicates an underestimation of the pre-ablation samples dimensions: from the tables it is possible to notice that the model tends to underestimate the initial samples dimension, preferable than overestimation willing to guarantee the complete ablation of the targeted tissue, and thus ensure the destroying of the whole tumor.

4. Conclusions

In this paper, the analytical predictive model proposed in [13] for the tissue shrinkage estimation *ex vivo* has been tested and validated on the results of experiments conducted with three commercially available MTA systems. The model succeeded in estimating the pre-

Table 1. Average, minimum and maximum error observed in applying the model to the Acculis™ results.

Acculis	15 mm side cubes			20 mm side cubes			30 mm side cubes			40 mm side cubes		
Irradiation time	***Avg [mm]***	***Min [mm]***	***Max [mm]***	***Avg [mm]***	***Min [mm]***	***Max [mm]***	***Avg [mm]***	***Min [mm]***	***Max [mm]***	***Avg [mm]***	***Min [mm]***	***Max [mm]***
1 min	1	-1	3	2	1	3	2	1	3	1	-3	5
2.5 min	0	-1	2	2	1	4	3	1	4	2	1	3
5 min	0	-1	1	2	0	4	1	-3	3	0	-3	4
7.5 min	0	-1	2	0	-2	1	1	0	3	0	-2	4
10 min	-1	-2	1	0	-2	2	0	-3	1	1	-3	4

Table 2. Average, minimum and maximum error observed in applying the model to the Amica™ results.

Amica	20 mm side cubes			30 mm side cubes			40 mm side cubes		
Irradiati-on time	***Avg [mm]***	***Min [mm]***	***Max [mm]***	***Avg [mm]***	***Min [mm]***	***Max [mm]***	***Avg [mm]***	***Min [mm]***	***Max [mm]***
1 min	-1	-2	2	1	-3	4	-1	-4	3
2.5 min	-2	-3	0	1	-4	3	-2	-3	-1
5 min	-1	-3	1	0	-3	3	-3	-7	1
7.5 min	-1	-3	1	0	-3	4	-3	-6	0
10 min	-1	-3	1	1	-3	4	-3	-6	-1

Table 3. Average, minimum and maximum error observed in applying the model to the Emprint™ results.

Emprint	20 mm side cubes			30 mm side cubes			40 mm side cubes		
Irradiati-on time	***Avg [mm]***	***Min [mm]***	***Max [mm]***	***Avg [mm]***	***Min [mm]***	***Max [mm]***	***Avg [mm]***	***Min [mm]***	***Max [mm]***
5 min	0	-3	1	0	-2	1	-1	-4	2
7.5 min	0	-3	1	-3	-7	1	-1	-2	-1
10 min	-1	-3	2	-3	-8	-1	-2	-5	1

ablation dimension of the treated tissue samples independently from the adopted device. Nevertheless, it has to be noted that the model is applicable only when carbonization occurs. In absence of charred tissue, the model does not adequately estimate the shrinkage, due to the possibly different thermal profile induced by the thermal ablation system. Further studies should be conducted to fully characterize the tissue shrinkage and improve the predictive model to make it widely applicable.

5. Acknowledgements

The authors acknowledge AngioDynamics, HS Hospital Service, and Covidien for having made available the MW antennas and the power generators. The authors alone are responsible for the content and writing of the paper.

This project has received funding from the European Union's Horizon 2020 research and innovation programme under the Marie Skłodowska-Curie grant agreement No 713690.

6. Disclosure stetement

Prof. Goldberg is both a consultant to and receives research support from Cosman Instruments and AngioDynamics.

7. References

1. R.Z. Swan, D. Sindram, J.B Martinie, and D.A. Iannitti, "Operative microwave ablation for hepatocellular carcinoma: complications, recurrence, and long-term outcomes," *J. Gastrointest. Surg.*, **17**, 2013, pp. 719, doi: 10.1007/s11605-013-2164-y

2. M.F. Meloni, S. Galimberti, and C.F. Dietrich, S. Lazzaroni, S.N. Goldberg, A. Abate, S. Sironi, and A. Andreano, "Microwave ablation of hepatic tumors with a third generation system: locoregional efficacy in a prospective cohort study with intermediate term follow-up," *Z. Gastroenterol.*, **54**, 2016, pp. 541–547, doi: 10.1055/s-0042-100627

3. M. Ahmed, C.L. Brace, F.T. Lee Jr, and S.N. Goldberg, "Principles of and advances in percutaneous ablation," *Radiology*, **258**, 2011, pp. 351–69, doi: 10.1148/radiol.10081634

4. V. Lopresto, R. Pinto, and M. Cavagnaro, "Experimental characterisation of the thermal lesion induced by microwave ablation," *Int. J. Hyperthermia*, **30**, 2014, pp. 110–118, doi: 10.3109/02656736.2013.879744

5. A.U. Hines-Peralta, N. Pirani, P. Clegg, N. Cronin, T.P. Ryan, Z. Liu, and S.N Goldberg, "Microwave ablation: results with a 2.45-GHz applicator in ex vivo bovine and in vivo porcine liver," *Radiology*, **239**, 2006, pp. 94–102, doi: 10.1148/radiol.2383050262

6. R. Hoffmann, H. Rempp, L. Erhard, G. Blumenstock, P.L. Pereira, C.D. Claussen, and S. Clasen, "Comparison of four microwave ablation devices: an experimental study in ex vivo bovine liver," *Radiology*, **268**, 2013, pp. 89–97, doi: 10.1148/radiol.13121127

7. S. Ganguli, D.D. Brennan, S. Faintuch, M.E. Ryan, and S.N. Goldberg, "Immediate renal tumor involution after radiofrequency thermal ablation," *J. Vasc. Interv. Radiol.*, **19**, 2008, pp. 412–418, doi: 10.1016/j.jvir.2007.10.024

8. C.L. Brace, T.A. Diaz, J.L. Hinshaw, and F.T. Lee Jr, "Tissue contraction caused by radiofrequency and microwave ablation: a laboratory study in liver and lung," *J. Vasc. Interv. Radiol.*, **21**, 2010, pp. 1280–1286, doi: 10.1016/j.jvir.2010.02.038

9. L. Farina, N. Weiss, Y. Nissenbaum, M. Cavagnaro, V. Lopresto, R. Pinto, N. Tosoratti, C. Amabile, S. Cassarino, and S.N. Goldberg, "Characterisation of tissue shrinkage during microwave thermal ablation," *Int. J. Hyperthermia*, **30**, 2014, pp.419–428, doi: 10.3109/02656736.2014.957250

10. V. Lopresto, R. Pinto, L. Farina, and M. Cavagnaro, "Treatment planning in microwave thermal ablation: clinical gaps and recent research advances," *Int. J. Hyperthermia*, **33**, 2017, pp. 83–100, doi: 10.1080/02656736.2016.1214883

11. D. Liu, and C.L. Brace, "CT imaging during microwave ablation: analysis of spatial and temporal tissue contraction," *Med. Phys.*, **41**, 2014, pp, 113303-1–9, doi: 10.1118/1.4897381

12. C.M. Sommer, S.A. Sommer, T. Mokry T, T. Gockner, D. Gnutzmann, N. Bellemann, A. Schmitz, B.A. Radeleff, H.U. Kauczor, U. Stampfl, and P.L. Pereira, "Quantification of tissue shrinkage and dehydration caused by microwave ablation: experimental study in kidneys for the estimation of effective coagulation volume," *J. Vasc. Interv. Radiol.*, **24**, 2013, pp. 1241–8, doi: 10.1016/j.jvir.2013.04.008

13. C. Amabile, L. Farina, V. Lopresto, R. Pinto, S. Cassarino, N. Tosoratti, S.N. Goldberg, and M. Cavagnaro, "Tissue shrinkage in microwave ablation of liver: an ex vivo predictive model," *Int. J. Hyperthermia*, **33**, 2017, pp. 101–109, doi: 10.1080/02656736.2016.1208292

14. L. Farina, Y. Nissenbaum, M. Cavagnaro, and S.N. Goldberg, "Tissue shrinkage in microwave thermal ablation: comparison of three commercial devices," *Int. J. Hyperthermia*, Published online August 2017, doi: 10.1080/02656736.2017.1362115

15. Acculis MTA System, products' specifications. http://www.angiodynamics.com/products/Acculis [accessed Feb 2016].

16. AMICA™, products' specifications. http://www.hshospitalservice.com [accessed Feb 2016].

17. AM. Ierardi, A. Mangano, C. Floridi, G. Dionigi, A. Biondi, E. Duka, N. Lucchina, GD. Lianos, and G. Carrafiello, "A new system of microwave ablation at 2450 MHz: preliminary experience," *Updates Surg*, **67**, 2015, pp. 39–45, doi: 10.1007/s13304-015-0288-1

18. Emprint™, products' specifications. http://www.medtronic.com/covidien/products/ablation-systems/ emprint-ablation-system [accessed Feb 2016].

19. L. Farina, V. Lopresto, R. Pinto, and M. Cavagnaro, "Microwave thermal ablation: performed studies and research needs," International Conference on Electromagnetics in Advanced Applications (ICEAA), 2017, doi: 10.1109/ICEAA.2017.8065313